Physics of Atomic Nuclei, Vol. 57, No. 9, 1994. From Yadernaya Fizika, Vol. 57, No. 9, 1994.

135

NAN'93

Proceedings of the Second Biennial Workshop on Nucleon–Antinucleon Physics Institute for Theoretical and Experimental Physics, Moscow, Russia September 13 - 18, 1993

Edited by
Yu. Kalashnikova, L. Kondratyuk,
A. Kudryavtsev, and N. Smorodinskaya
(ITEP)

Physics of Atomic Nuclei, Vol. 57, No. 9, 1994, pp. 1635 - 1644. From *Yadernaya Fizika*, Vol. 57, No. 9, 1994, pp. 1705 - 1714.

$\bar{N}$-NUCLEUS INTERACTION

Nuclear Multifragmentation: Antiprotons versus Photons and Heavy Ions*

J. Cugnon[1)]

Abstract – Nuclear multifragmentation is the phenomenon by which a nucleus breaks into many pieces of intermediate size. It occurs in the excitation-energy regime, between the spallation + evaporation regime and the explosive fragmentation regime. The various models of multifragmentation are briefly reviewed and the possibility of critical behavior in the multifragmentation process is underlined. Unanswered problems are stated. It is shown, by model calculations, that antiproton annihilation is, in many respects, better suited than proton–nucleus and heavy-ion collisions for studying multifragmentation and, in other respects, complementary to these other tools.

1. INTRODUCTION

Antiproton annihilation on nuclei in the LEAR regime leads to target fragmentation. This possibility, which was perhaps overemphasized at the beginning of LEAR activity [1], has been demonstrated by [2] and [3] in which the residue mass spectrum was measured. In the case of annihilation at rest on a ^{98}Mo target, up to 32 nucleons can be removed from the target [2]. For heavy targets, fission is also possible [4]. These observations are well explained and illustrated by the intranuclear-cascade (INC) model [5 - 7]. According to the latter, the incoming antinucleon annihilates on a single target nucleon at the surface of the nucleus, giving birth to a few pions, which may escape readily, scatter with the target nucleons, or be absorbed on the target. This is illustrated by Fig. 1. In this process, the flow of energy from the pionic system to the (baryonic) target system shows three different time scales, as depicted in Fig. 1: the pionic system transfers quickly around 500 MeV (at rest) to the target; the latter dissipates the largest part of it in a short time scale (~30 fm/c) by emission of fast particles (mostly nucleons, but also deutons, ...); afterwards, the remaining excitation energy of the more or less thermalized nucleus is released on a much longer time scale in a manner that resembles ordinary evaporation. The entire process can be characterized as a multispallation (induced by several pions ejecting a few fast particles) followed by evaporation that leaves a heavy residue; this is very much akin to what occurs when a fast particle hits a nucleus. We must realize that the mass loss is largely due to the evaporation. This is illustrated in Fig. 2.

The spallation + evaporation scheme is typical of a low-energy regime, where the excitation energy provided to the target is rather low. If the excitation energy is increased (to an amount that will be discussed below), it is believed that the target may fragment into many pieces. This is the so-called multifragmentation. Our main goal in this paper is twofold. First, we want to summarize the aspects and the issues of multifragmentation as revealed by previous studies. Second, we want to discuss the respective merits (and drawbacks) of the antiproton as a tool for studying multifragmentation and to compare the antiproton with other possible probes, the proton and heavy ions.

2. THE ISSUES OF NUCLEAR MULTIFRAGMENTATION

2.1. Definition

When a nucleus is bombarded by any massive projectile (at low energy), it loses a few fast nucleons by spallation and several slow ones by evaporation. There is, in any case, a big target residue, of a size comparable to the one of the target.

Conversely, in violent collisions, as in heavy-ion experiments in the GeV/u domain [8], the system is highly excited and explodes into many small pieces, basically nucleons.

In the intermediate energy regime, it is expected that the system breaks into many intermediate-mass fragments (IMF), whose size is not comparable with the target mass. There is no precise definition of the IMFs, but it is customary to define them as having a mass between ~4 to ~40 for a heavy target (Au, Pb, ...). As a guiding line, we may think of the target excitation energy at the end of the fast-ejection (or preequilibrium) process (we denote it hereafter by E^*) as the parameter that determines the way in which the nuclear system fragments. The main regimes of fragmentation are depicted in Fig. 3: as E^* increases, we pass from the spallation + evaporation to the multifragmentation, and finally, to the explosion regimes. To give an approximate idea, the transition from spallation + evaporation to multifragmentation would occur when E^* is between 3 and 5 MeV per nucleon, and the explosion regime would appear when the excitation energy per nucleon approaches the average binding energy, i.e., ~8 MeV. The precise transition points are not yet known. The fact that the transitions are sharp is still largely

* This article was submitted by the author in English.

1) Université de Liège, Institute of Physics B5, Sart Tilman, B-4000 Liège 1, Belgium.

1063-7788/94/5709-1635$10.00 © 1994 МАИК Наука/Interperiodica Publishing

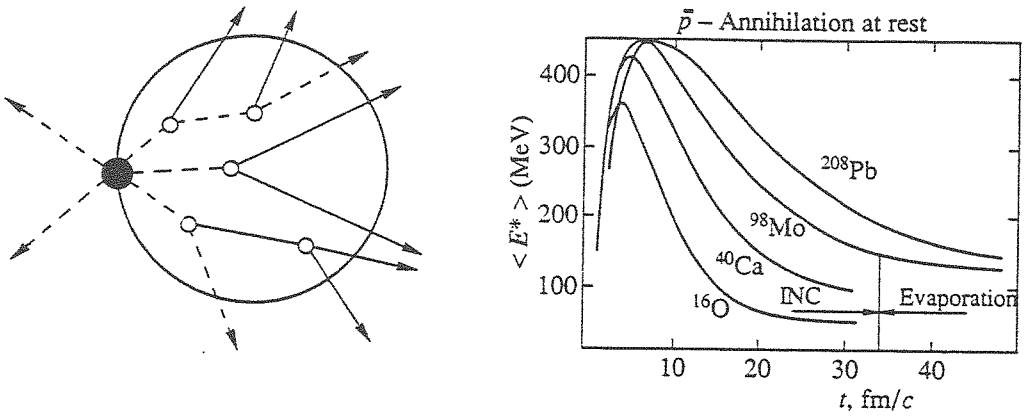

Fig. 1. Left: schematic representation of antiproton annihilation on a nucleus. Right: time evolution of the target excitation energy, as predicted by the INC model.

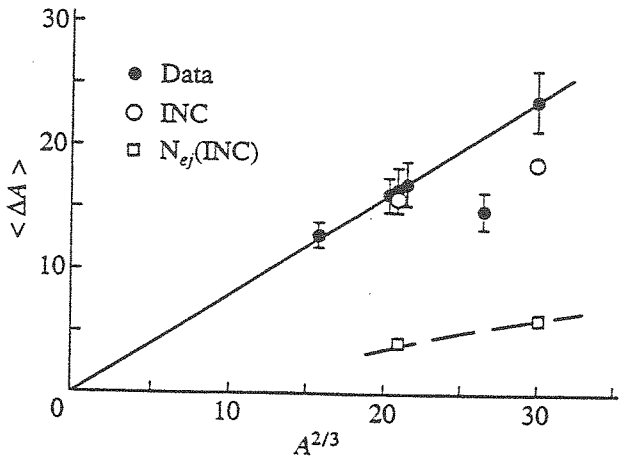

Fig. 2. Average target mass loss after antiproton annihilation as a function of the target mass raised to a power of 2/3: experimental data of [3] (dots) and INC predictions of [5] (open circles). The contribution to the mass loss due to the fast ejection process, as predicted by the INC model, is given by the open squares.

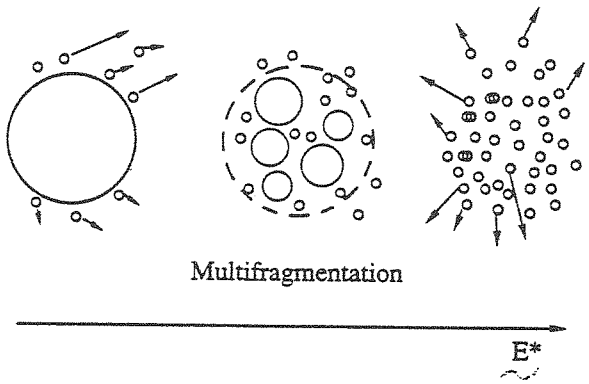

Fig. 3. Schematic representation of the three regimes of nuclear fragmentation in their order of appearance with increasing excitation energy E^*: spallation–evaporation, multifragmentation, and explosion. The dashed curve indicates the size of the original target.

a conjecture and the possibility of investigating this pattern heavily relies on the possibility of achieving (at least to some degree) thermalization in the course of the collision process and on a method for measuring or evaluating E^* when thermalization is complete.

2.2. *Observation of Multifragmentation*

Multifragmentation events have been observed in heavy-ion reactions (see, e.g., [9] for a review) as well as in proton–nucleus collisions [10]. Figure 4 shows the increase of the measured IMF production in these two systems as a function of the bombarding energy. The cross section for the IMF production becomes a sizeable part of the reaction cross section.

Furthermore, in a given experiment, the IMF multiplicity has also been measured as a function of certain parameters that are supposed to vary monotonically as a function of the impact parameter (with unknown fluctuations). Figure 5 shows two examples. In the first case, the chosen variable is the deposited energy, estimated theoretically from a certain transport code. In the second case, it is the total charge that appears in composites and not in free protons. Both variables are expected to vary monotonically with the impact parameter and with the excitation energy, with some fluctuations of course.

2.3. *Questions and Issues*

There are mainly three unanswered questions or issues concerning multifragmentation:

(1) The onset of multifragmentation is a smooth function of the experimental variables, i.e., the bombarding energy E_{lab} and the impact parameter b (see above). However, it is conceivable (and theoretically expected) that the onset is sharp in terms of the excitation energy E^* or in terms of some other relevant variables. It must be stressed that, due to the complexity of the reaction process, the kinematic variables (E_{lab}, b) do

not determine the excitation energy uniquely: there are presumably many fluctuations on E^* [11]. This conjecture should be checked and the related questions should be raised: Is there a possibility to measure E^*? Is there any other more relevant variable?

(2) There is another important effect of the fluctuations: the fragmenting system, i.e., the part of the total system that may be considered as thermalized and that undergoes a subsequent fragmentation, is not always the same for a given value of the kinematic variables (E_{lab}, b). This is evident for antiproton annihilation on nuclei at rest, since the number of ejected nucleons fluctuates from one event to the other [12]. This is even more true for heavy ions, where the collision process is much more complicated (see below). The question arises of knowing the size and the properties of the fragmenting system. This question is totally unanswered in the heavy-ion case.

(3) More basically, we may address the following question: What is the cause of multifragmentation? We will briefly review the most up-to-date models.

The first class of models is based on statistical decay [13, 14]. It assumes that the fragmentation of an excited system of A nucleons in a volume V at temperature T is governed by phase space. The basic theoretical quantity is then the partition function

$$Z(V, T, A) = \sum_{\substack{\text{all partitions:} \\ \sum_f n(A_f)A_f = A}} V^{\sum_f n(A_f)} e^{-\beta E_{part}}, \qquad (2.1)$$

where the sum runs over all partitions of the system in $n(1)$ fragments of mass number A_1, $n(2)$ fragments of mass number A_2, ...; and where E_{part} is the sum of the energy of the fragments in the corresponding partition. For more detail, see [13]. The average number of fragments of size A_f is then given by

$$\langle n(A_f)\rangle = \frac{1}{Z}\sum n(A_f) V^{\sum_f n(A_f)} e^{-\beta E_{part}}, \qquad (2.2)$$

where the summation is the same as before. Any correlation function and the fluctuations of any quantity can be calculated accordingly. They are of course typical of the canonical ensemble. Prior to any calculation, we must complement this model with a prescription that relates T and V to E_{lab} and b, and possibly to E^*. This raises a serious problem. Nevertheless, this type of model predicts a regime of E^* where multifragmentation dominates over evaporation and fission. The onset is smooth in this case [13].

The second class of models relates multifragmentation to a gas–liquid instability [15, 16]. The bulk of nuclei is made of a matter (the "nuclear matter") at nucleon density ~0.17 fm^{-3}. This matter has a phase diagram, which is depicted in Fig. 6, typical of a Van der Waals fluid. In nuclei, this matter is at equilibrium ($p = T = 0$) and in the liquid phase. In a collision process, the nuclear matter is heated and possibly

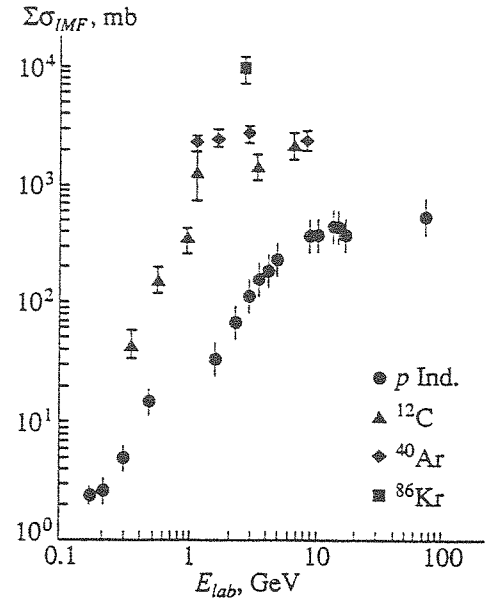

Fig. 4. IMF production cross section as a function of the laboratory projectile energy in proton–nucleus collisions (heavy dots) and in some heavy ion reactions (adapted from [33]).

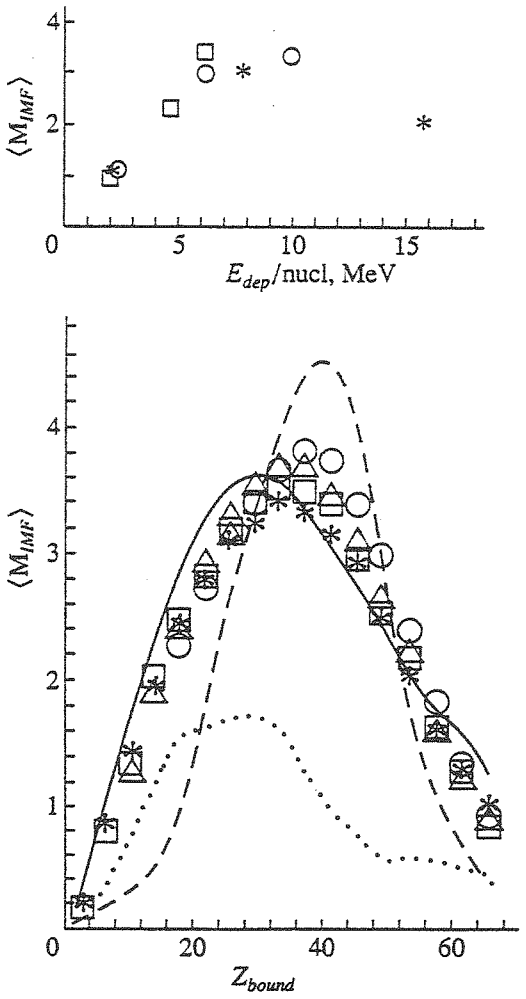

Fig. 5. Average multiplicity of IMF as a function of some parameters that are supposed to vary monotonically with E^* (see text) (adapted from [19]).

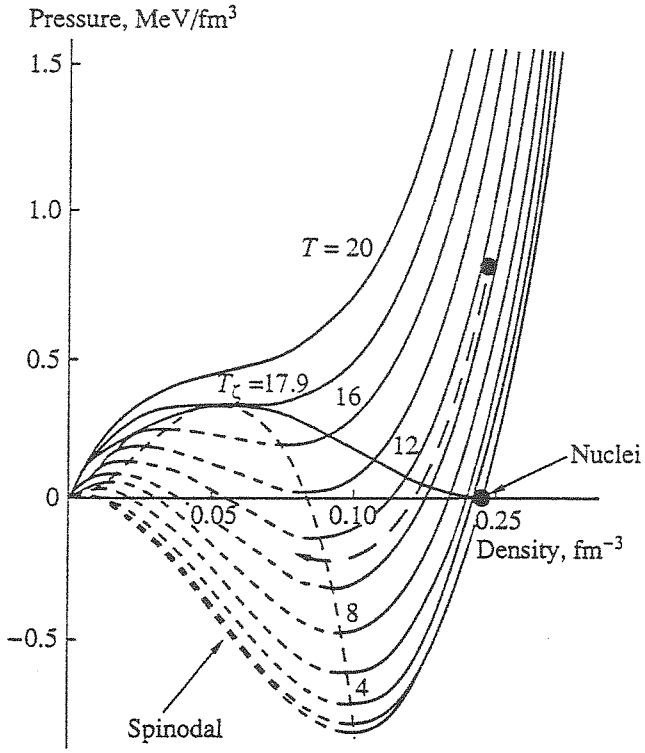

Fig. 6. Isotherms of nuclear matter for various temperatures T indicated along the curves in MeV. The ordinary nuclei correspond to the point $p = T = 0$. The dotted line represents the expansion of an excited nuclear system (see text).

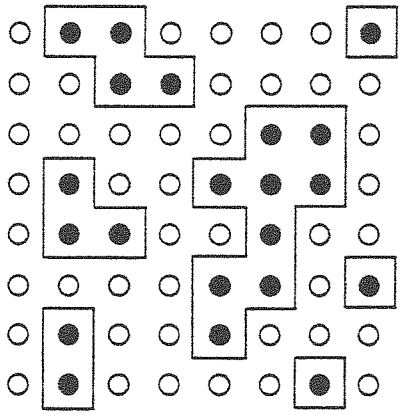

Fig. 7. Percolation on a two-dimensional lattice. The broken lines enclose the clusters (see text).

compressed and can be represented by the heavy dot in the upper part of Fig. 6. Due to the positive pressure, the matter will expand, following the indicated path in Fig. 6. Ultimately, depending upon the excitation energy, the path enters the spinodal (dotted area), where the compression coefficient

$$\kappa = (\partial p/\partial V)_T = -\frac{\rho}{V}\left(\frac{\partial p}{\partial \rho}\right)_T \qquad (2.3)$$

is positive. In these conditions, the matter becomes unstable under density fluctuations. Any fluctuation grows freely, voids appear inside the matter, and finally, fragmentation occurs. The instability involves the bulk of the matter and thus leads to the fragmentation of the system into many pieces. This kind of model likely leads to a sudden onset of multifragmentation, although this feature has only rarely been investigated quantitatively.

The third class of models borrows arguments from percolation theory. In its simplest version, percolation theory looks for geometrically constructed clusters on a lattice where a fraction $1-p$ of the sites has been removed at random (see Fig. 7). This model shows a phase transition (at $d \geq 2$ dimensions). For large p, there is always a big cluster (the percolating cluster) that roughly extends over the entire lattice. Suddenly, at some value $p = p_c$, this large cluster disappears, and for $p < p_c$, there are only small clusters (much smaller than the original lattice). Actually, this model provides a simple picture of the conductor–insulator transition and of many other phenomena [17]. The average distribution of the cluster sizes also changes drastically when p changes through p_c. For $p > p_c$, there is one large and many very small clusters. As p decreases, the gap is progressively filled up, and at $p = p_c$ (0.45 in the case of Fig. 8), the large clusters disappear and the size distribution is rather broad. If p is very small, there are only small clusters. It is tempting to relate these features with the various regimes of nuclear fragmentation, assuming that a fraction $1-p$ of the nucleons has been removed by the fast process, or more loosely assuming a monotonous relation between p on E^*: large p corresponds to the evaporation regime, $p \approx p_c$ corresponds to the multifragmentation, and small p corresponds to explosive fragmentation.

Although very crude, this model is surprisingly successful (after a fitting of the parameter p on the data); it is more successful than the other approaches (for recent results, including correlations between fragments, see [18, 19]). This raises a real puzzle, since it is a purely geometrical model, apparently deprived of dynamics. The explanation may lie in the fact that it displays critical phenomena. In all generality, critical phenomena are those phenomena (involving an extended system) that occur when an external parameter approaches a critical value. They can be summarized as follows:

(1) there exists an order parameter that assumes two radically different values when the external parameter is varied;

(2) discontinuities appear in some physical quantities;

(3) the correlation length becomes very large near the critical point;

(4) fluctuations become very large near the critical point;

(5) scaling laws are observed;

(6) universality appears; some features are independent of the detail of the dynamics, and roughly speaking, depend only upon the dimensionality of the system.

For the percolation transition, the order parameter is the size A_p of the percolating cluster. Close to p_c, it goes like

$$A_p \propto (p - p_c)^\alpha \qquad (2.4)$$

for p going down to p_c, where σ is a critical exponent less than unity, indicating a strong discontinuity in the slope of A_p in function of p. The r-space correlation length ξ, i.e., the length up to which we can travel from an occupied site to find sites occupied with a large probability, goes to infinity near the critical point $p = p_c$ (more exactly, it becomes very large for finite lattices). Fluctuations also become very large near the critical point (infinite for an infinite lattice): not only $n(A_f)$, but the entire cluster size distribution strongly fluctuates. The latter fluctuations are conveniently described by the fluctuations of the moments of the cluster distribution; for example, the (reduced) second moment diverges at $p = p_c$ [20]. The cluster distribution scales (in $d = 3$ dimensions) as

$$n(A_f) = NA^{(D-3)/3} f\left(\frac{A_f}{A^{D/3}}, p\right), \qquad (2.5)$$

where N is a normalization constant, A is the original size of the system, and D is some fractal dimension typical to the percolation model. In (2.5), the function f is given by

$$f(s, p) = s^{-\tau} g\left(\frac{s}{|p - p_c|^{1/\sigma}}\right), \qquad (2.6)$$

where g is a function that goes to unity when $p \longrightarrow p_c$. Thus, in the same limit, the cluster distribution looks like (see Fig. 8)

$$n(A_f) \sim A_f^{-\tau}, \qquad (2.7)$$

where τ is a critical exponent, independent of the size of the system. Universality corresponds to an independence of relations (2.4) - (2.6) to the type of the lattice for a given dimension.

Finally, let us mention that many different systems with different dynamics show the same critical behavior, the latter arising only from some restricted property of the dynamics and from the dimension of the system. Those systems are said to belong to the same class of universality (see [21] for a discussion of this feature).

We may speculate that the success of the percolation model in describing nuclear fragmentation is due to its ability to exhibit critical behavior in a simple and transparent manner. Very likely, the percolation model has simply picked up the correct class of universality. Of course, the correct picture of multifragmentation needs more dynamical insight. Here, we have in mind the spinodal decomposition models. However, the critical behavior of this kind of model must still be worked out. Although it is rather clear on physical grounds that the spinodal decomposition is able to generate critical behavior [22], the study of the latter will be difficult, since then we must deal with dynamic (i.e., time-dependent) critical phenomena, which are not as well documented as static ones.

2.4. A Possible Strategy

The basic questions to be answered are, in our opinion, the following: what is the mechanism of multifragmentation? does it show critical behavior in terms of a suitable parameter? what is this parameter?

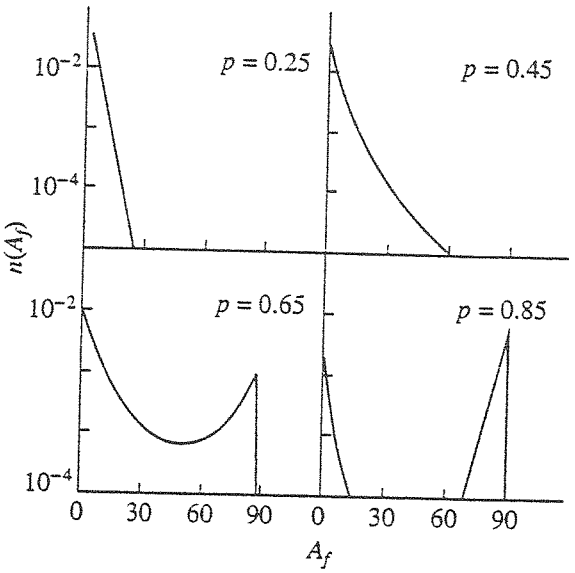

Fig. 8. Cluster-size distribution in a three-dimensional percolation model with 100 original sites, as a function of the parameter p (see text).

Obviously, the answer to these questions requires the study of the fluctuations, and therefore, event-by-event measurements. The first task is to isolate critical behavior. In heavy ions, this has partly been achieved [20]. There is some hint to critical behavior, but the latter is not clearly evident, presumably because the fragmenting system is not clearly defined in that case (see Section 3). Intermittency analysis can also be useful for exhibiting critical behavior [23, 24]. Hopefully, we may be able to identify the class of universality to which multifragmentation belongs. Finally, we should check with theoretical models that are supposed to generate critical behavior. Clearly, in order to carry this program with success, we need to study systems in which the fragmenting system is well defined. We will show in the next section that antiprotons may be very helpful in this respect.

3. COMPARISON BETWEEN ANTIPROTONS, PROTONS, AND HEAVY IONS

3.1. Introduction

Obviously, the onset of multifragmentation has been observed in proton and in heavy-ion induced reactions (see Fig. 4). The explosive regime has been observed in heavy-ion collisions in the GeV/u regime. For protons, no explosive regime has been clearly demonstrated and, in any case, would appear at several GeV. Here we want to make precise the regime of multifragmentation for antiprotons (and accessorily for the other probes). Obviously, annihilation at rest corresponds to the subcritical (spallation + evaporation) regime, as illustrated in Fig. 9, which shows the target residue mass spectrum in this case. In order to investigate the

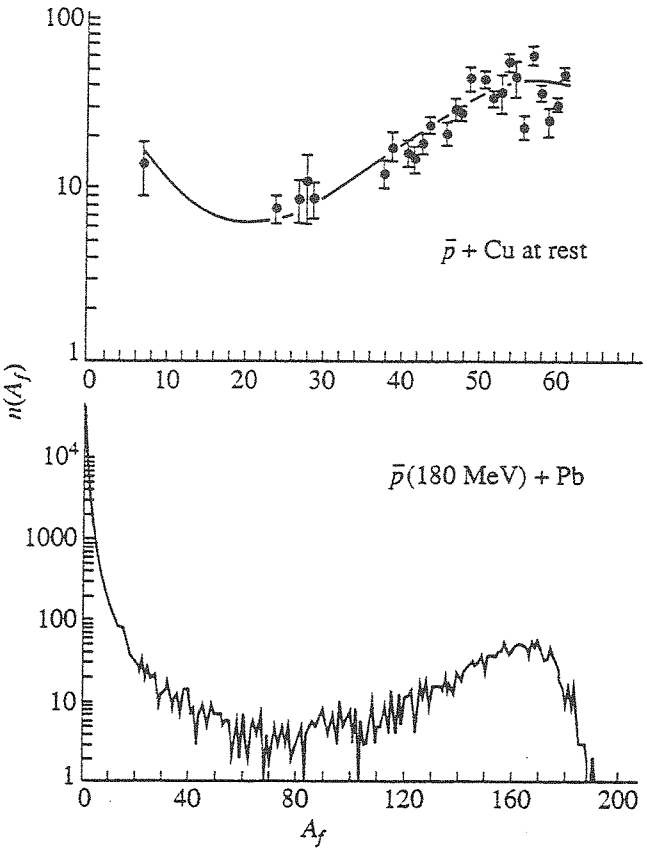

Fig. 9. Top: residue mass spectrum (in arbitrary units) following antiproton annihilation on Cu at rest (adapted from [3]). Bottom: the same quantity for low-energy antiproton annihilation on Pb, as predicted by the INC + percolation model.

multifragmentation in various systems, we will use the INC + percolation model. In this approach, the cascade is stopped at the end of the fast process and a percolation procedure is applied on the configuration of the system at that time; if two nucleons are separated by a distance smaller than a parameter d_{cut}, they belong to the same cluster, and the cluster decomposition is built in this way. This model has given reasonable agreement for the cluster-size distribution in proton and heavy-ion reactions [25]. It can at least serve for a first investigation of the gross properties of multifragmentation. For low-energy antiproton annihilation, the model gives a characteristic U-shape for the mass distribution, which reproduces the observed residue-mass spectrum (Fig. 9).

Before studying the kinematical conditions required for multifragmentation in antiproton–nucleus, proton–nucleus, and heavy-ion systems, we will study the characteristics of the fragmenting system.

3.2. Comparison between the Various Systems

We will successively study the following aspects:

(1) Homogeneity of the Fragmenting System

This has been studied in the antiproton–nucleus [26] and proton–nucleus [11] systems. In both cases, after a brief boring phase (more pronounced in the proton case), the nucleus again becomes more or less homogeneous at the end of the fast process. For the heavy-ion case, illustrated in Fig. 10, the system is more complicated; at the end of the hard collision process (~ 40 fm/c), the system can be divided roughly into three parts, namely, a very hot central part and two "cold" spectator parts, which correspond to the parts of the projectile and the target that have not been intercepted by the other partner. At lower energy, the mixing of the systems is even more important [27].

(2) Thermalization of the Fragmenting System

It is, of course, important that some degree of thermalization (or at least randomization) be achieved; otherwise, it would be difficult to speak about the fragmenting system itself and of the fragmentation in terms of macroscopic properties of the system. There are several theoretical ways to investigate this point (in some heavy ion collisions, this could even be checked experimentally [27]). One way is to look at the emission pattern of the evolving system. For instance, in Fig. 11, we plotted the forward–backward ratio for the nucleon emission at the end of the hard process in the proton–nucleus and antiproton–nucleus systems. We see that the situation, although not ideal, is better for antiprotons. We recall that in central heavy ions the situation is even better [27]. For noncentral collisions, the mixing of different fragmenting subsystems shows up, as we explained above.

(3) Transferred Energy and Excitation Energy

In central heavy-ion reactions (for symmetric systems at least), in the GeV/u range, the matter-stopping power is very high [8]. Therefore, a large extent of the available c.m. energy is transformed into excitation energy [8, 28]. In the proton–nucleus case, the situation is illustrated by Fig. 12. Let us recall that we can write, in that case,

$$\begin{aligned} W_p^0 &= W_p + W_{transf} \\ &= W_p + W_{ej} + E^* + (W^0_{remnant} - W_t^0), \end{aligned} \tag{3.1}$$

where W_p^0 and W_p are the initial and final proton energies, W_{ej} is the energy of the ejectiles, $W^0_{remnant}$ and W_t^0 are the ground state energies of the remnant and the target, respectively, and E^* is the remnant excitation energy. Following our discussion of Section 2, the relation (3.1) should be considered as representing the partition of the energy at the end of the fast process. We see from Fig. 12 that, if the transferred energy can be very large, the excitation energy is only a small fraction of it. The situation for the antiproton case is depicted in Fig. 13. A relation similar to (3.1) holds, where W_p^0 and W_p should be replaced by the energy of the primordial pions (the annihilation energy) and that of the final pions, respectively. We see that antiprotons are

more advantageous for generating excitation energies at a given incident energy E_{lab}. This feature is even more nicely illustrated by Fig. 14, where the excitation energies reached in the three systems are compared to each other as functions of the incident energy per baryon. It is believed, on the basis of existing observations [29] and models [30], that multifragmentation occurs for excitation energy of ~3 - 6 MeV per nucleon. This is indicated on the vertical scale of Fig. 14 for nuclei around mass 200. It can be seen that the average value of 5 MeV is reached with heavy ions at moderate energy (~100 MeV/u, a domain covered or almost covered by existing accelerators at GSI, GANIL, SATURNE, ...), with antiprotons of 1 - 2 GeV incident energy (which could be covered by LEAR), and with protons of incident energy larger than, say, 4 GeV.

The situation is then more favorable for antiprotons than for protons. The change of the fragmentation pattern when going from low energy to a few-GeV antiprotons was studied with the INC + percolation model in [31]. Because of the lack of space, we will not reproduce these results here. Basically, the bump observed for large fragments in Fig. 8 tends to disappear above ~1 GeV, and the IMF part of the mass spectrum, i.e., for $1 < A_f \leq 35$, shows a typical effective power law

$$n(A_f) \sim A_f^{-\tau_{eff}}, \qquad (3.2)$$

where the effective exponent τ_{eff} changes with the incident energy in a way that is depicted in Fig. 15. Clearly, there is a drastic change for antiprotons around 1 GeV, which indicates a steeper and steeper decrease of the spectrum in this A_f mass range, as the energy increases (it should be compared to the critical behavior of the percolation model, see Fig. 7). Let us also notice in Fig. 15 the less favorable behavior of the proton case. The INC + percolation model also predicts different behaviors, in the proton and antiproton cases, of the mass of the percolating cluster, i.e., of the mass of the percolating cluster and of the fluctuations in the spectrum, as the energy increases [32]. Both features point to a critical behavior in the antiproton case between 1 and 2 GeV.

(4) Linear Momentum Transfer

In heavy ions, the momentum acquired by the fragmenting system may be very large. This is rather embarrassing, but may sometimes be turned to advantage when an experiment is performed in the so-called inverse kinematics with a good detecting system in the forward direction. The situation in the proton–nucleus and antiproton–nucleus cases may be investigated with the INC model. The linear momentum of the remnant is shown in such an approach by Fig. 16. Surprisingly, the remnant momentum does not vanish at low incident energy in the antiproton case. The explanation lies in the fact that annihilation takes place on the surface; pions emitted backwards escape readily, whereas pions emitted in the forward direction transfer a part of their momentum to the remnant. The momentum transfer is

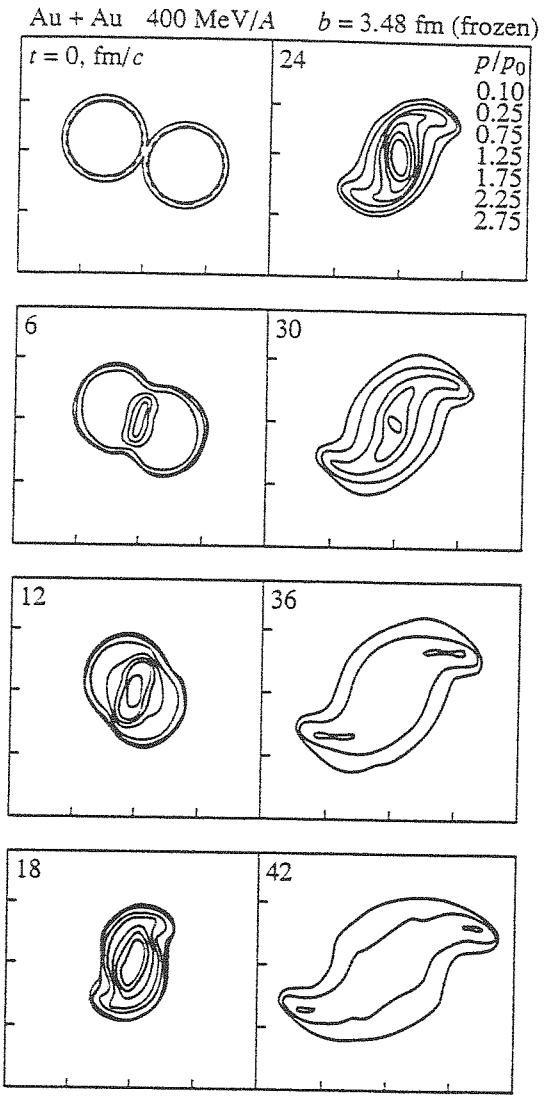

Fig. 10. Nucleon-density profile (in the c.m. frame) during an Au + Au collision at b = 3.48 fm. The time after the beginning of the collision is given in each square of the figure. At t = 0, the two nuclei are running against each other along the horizontal direction (adapted from [34]).

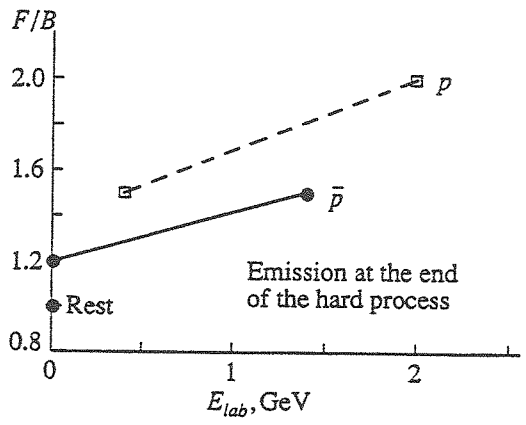

Fig. 11. Forward–backward ratio for nucleon emission at the end of the hard process in proton–nucleus collisions and antiproton annihilation on nuclei.

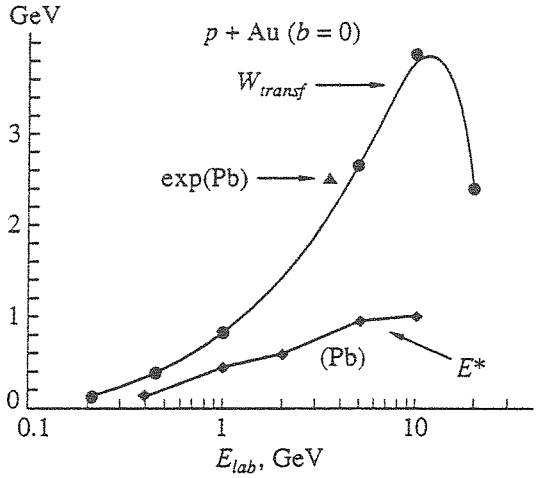

Fig. 12. Transferred energy in central collisions of protons with an Au target (upper curve) and excitation energy E^* (at the end of the fast process) in central collisions of protons with a Pb target. The experimental measurement of the transferred energy is taken from [35].

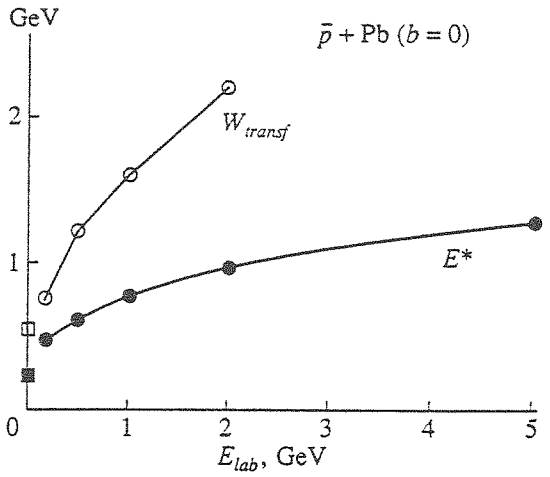

Fig. 13. Same as Fig. 12 for antiproton annihilation at small impact parameter. The squares correspond to annihilation at rest.

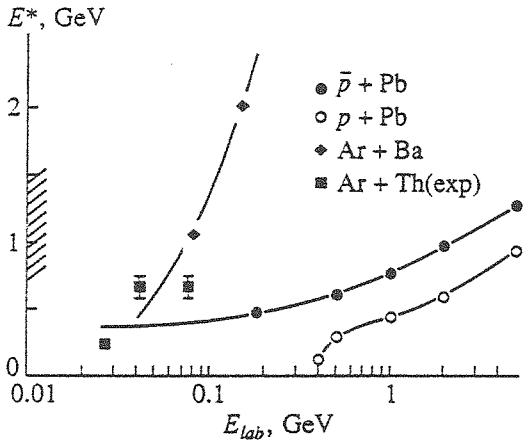

Fig. 14. Comparison of the excitation energy E^* at the end of the hard process for three different systems. The shaded area indicates the expected range of E^* for multifragmentation. The experimental data for Ar + Th are taken from [36].

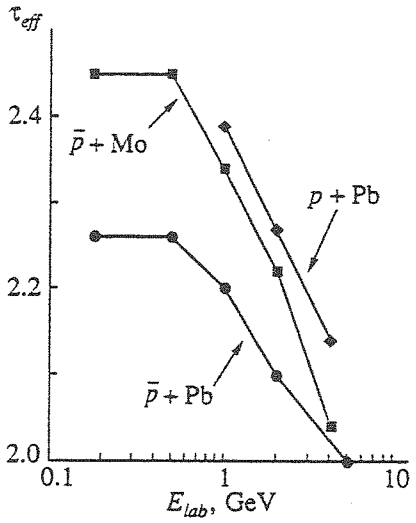

Fig. 15. Evolution of the effective exponent with the incident energy in three systems (see text).

roughly the same in the proton case for incident energy larger than ~1 GeV.

(5) Angular Momentum Transfer

The angular momentum transferred to the fragmenting system and of the excitation energy on the excitation energy on the impact parameter of the collision is shown in Fig. 17 for the three systems (at roughly the threshold for multifragmentation for Ar + Ba and $\bar{p}$ + Pb and at 2 GeV for p + Pb). Two features are worth noting. First, the angular momentum transfer is much larger in the heavy-ion case than in the two other cases and is the smallest in the antiproton case. Second, the impact parameter dependence of the excitation energy is quite large in the heavy-ion case and rather small in the antiproton case. Therefore, the latter appears very promising, since even without an impact parameter selection, it does not mix very different events. It is rather clear that this property comes from the isotropic emission of the pions in the annihilation.

3.3. Summary of the Comparison

The table gives an overview of the respective advantages and merits of the three systems under consideration for studying multifragmentation. Before discussing this point in more detail, it should be stressed that the comparison relies on the INC + percolation model adopted here. The first line gives just the incident energy corresponding to the onset of multifragmentation. The second line deals with the momentum transfer to the fragmenting system. In most of the current detectors, it is

preferable to have neither a momentum transfer too high nor a too low; what is most important is that we are able to detect and identify all of the (charged) particles issued from the multifragmentation. If these particles are too slow, they are below the kinematical cuts. If they are too fast, they may accumulate in the forward direction. The third line corresponds to the angular momentum of the fragmenting system. The difficulty here lies in the fact that the fragmentation may be very dependent upon the rotation of the system, as is the case for fission (which may be considered, after all, as the simplest form of fragmentation). Furthermore, if the angular momentum changes very much with the impact parameter, it is necessary to have a good impact parameter selector; otherwise, we mix different events with fragmenting systems with different properties.

The fourth line refers to the definition of the fragmenting system. As was already explained, it is better to have at the end of the fast process a fragmenting system of properties that do not fluctuate too much, and that is homogeneous and thermalized to the greatest extent possible. Of course, it would be of interest to study the fragmentation of excited unthermalized systems. But, mixing systems with different characteristics would make the analysis much more difficult. Furthermore, if at the end of the fast hard process, the system is composed of several subsystems of different characteristics (as is the case for heavy ions, see Fig. 7) and of different fragmentation properties, the analysis is rendered still more difficult, unless we can isolate the decay products of one of the subsystems. The situation is even worse if the system is a collection of many subsystems of smoothly varying characteristics. This possibility is shown in the next line of the table. Finally, the last line refers to a feature that we did not discuss here, namely, the possible compression of the fragmenting system. Antiproton annihilation yields a fragmenting system that is roughly at normal density [26], and therefore appears, from this point of view, as a complementary tool for studying multifragmentation.

4. CONCLUSION AND PROSPECTS

We have discussed the possibility of studying nuclear multifragmentation by means of antiproton annihilation on nuclei.

We want first to summarize the unanswered questions in multifragmentation in light of the previous studies with heavy ions. There is some hint that multifragmentation would correspond to a critical phenomenon. However, this has yet to be firmly established. The next unanswered question involves the physical cause of multifragmentation and what is (are) the physical parameter(s) that control(s) the appearance of multifragmentation. The best candidate up to now is the spinodal decomposition, which may generate critical behavior for a wide range of the density and temperature (or entropy) of the fragmenting system. Progress in the understanding of these questions demands both theoretical and experimental efforts. From the theory side,

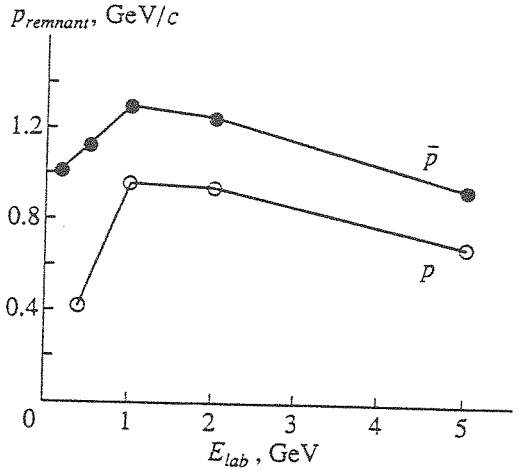

Fig. 16. Momentum of the remnant in central proton–nucleus and antiproton–nucleus interactions.

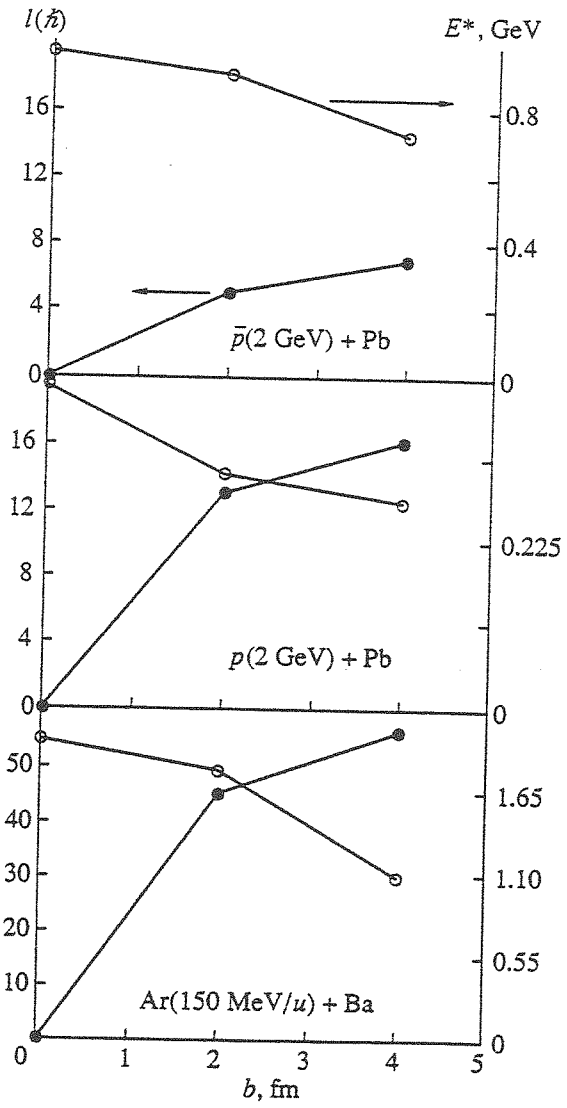

Fig. 17. Angular momentum l (left scale) and excitation energy E^* (right scale) of the remnant in the three indicated systems.

Comparison between different probes

	$\bar{p}$	Heavy ions	p
E_{crit}	1 - 2 GeV	~200 MeV/A	$\gtrsim$5 GeV
Momentum transfer	~Small	Large	~Small
Angular momentum transfer	Small	Large	~Small
Definition of the fragmenting system	Good	~Bad	Bad Good
Degree of thermaliation/homogenization	Good	~Bad	Bad Good
Compression	No	Yes	No Yes

the dynamic (i.e., time-dependent) critical behavior should be studied in detail in order to sort out the relevant external parameters. From the experimental side, the most obvious effort should deal with detailed study of the fluctuations. This, of course, requires the use of good 4π detectors.

Let us stress that the interest of multifragmentation (besides the practical interest of knowing how a nucleus breaks into pieces) lies in a possibly new type of critical behavior, which might be linked to a rapid expansion of the system, a feature that, as far as we know, has no counterpart in ordinary systems. It would be deceptive if the multifragmentation was explained by statistical models that include only simple properties of nuclei.

In Section 3, we investigated the advantages of antiprotons over the conventional tools of protons and heavy-ion beams in studying multifragmentation, namely, protons and heavy-ion beams. In summary, we can say that antiproton annihilation requires less incident energy, giving rise to a better homogenization and randomization of the fragmenting system. Furthermore, angular-momentum transfer is small and the impact parameter dependence is rather weak. All of these features lead to the expectation of a "well-prepared" fragmenting system, which should facilitate the analysis; whereas in the proton and heavy-ion cases the mixing of events of different fragmenting systems is, as expected, more important.

REFERENCES

1. Rafelski, J., *Phys. Lett. B*, 1980, vol. 91, p. 281.
2. Moser, E.F., Daniel, H., von Egidy, T., *et al.*, *Phys. Lett. B*, 1986, vol. 179, p. 25.
3. Jastrzebski, J., Kurcewicz, W., Lubinski, P., *et al.*, *Phys. Rev. C: Nucl. Phys.*, 1993, vol. 47, p. 216.
4. Machner, H., Sa Jun, and Riepe, G., *Z. Phys. A: At. Nucl.*, 1992, vol. 343, p. 73.
5. Jasselette, P., Cugnon, J., and Vandermeulen, J., *Nucl. Phys. A*, 1988, vol. 484, p. 542.
6. Hernández, E. and Oset, E., *Nucl. Phys. A*, 1986, vol. 455, p. 584.
7. Golubeva, Ye.S., Iljinov, A.S., Botvina, A.S., and Sobolevsky, N.M., *Nucl. Phys. A*, 1988, vol. 483, p. 539.
8. Nagamiya, S. and Gyulassy, M., *Adv. Nucl. Phys.*, 1984, vol. 13, p. 201.
9. *Proc. Fourth Int. Conf. on Nucleus–Nucleus Collisions, Kanazawa*, Toki, H., Tanihata, I., and Kamitsubo, H., Eds., Amsterdam: North-Holland, 1992.
10. Finn, J.E., Agarwal, S., Bujak, A., *et al.*, *Phys. Rev. Lett.*, 1982, vol. 49, p. 1321.
11. Cugnon, J., *Nucl. Phys. A*, 1987, vol. 462, p. 751.
12. Cugnon, J. and Vandermeulen, J., *Nucl. Phys. A*, 1985, vol. 445, p. 717.
13. Gross, D.H.E., *Nucl. Phys. A*, 1993, vol. 553, p. 175c.
14. Bondorf, J.P., Donangelo, R., Mishustin, I.N., and Schulz, H., *Nucl. Phys. A*, 1985, vol. 444, p. 460.
15. Cugnon, J., *Phys. Lett. B*, 1984, vol. 135, p. 374.
16. Friedman, W.A., *Phys. Rev. C: Nucl. Phys.*, 1990, vol. 42, p. 667.
17. Stauffer, D., *Phys. Rep.*, 1979, vol. 54, p. 1.
18. Leray, S. and Souza, S., *Preprint of Laboratoire National Saturne*, no. LNS/Th/93-16.
19. Lynen, U., Kreutz, P., Adloff, J.C., *et al.*, *Nucl. Phys. A*, 1992, vol. 545, p. 329c.
20. Campi, X., *J. Phys. A: Math. Nucl. Gen.*, 1986, vol. 19, p. L917.
21. Ma, S.K., *Modern Theory of Critical Phenomena*, Reading: Benjamin, 1976.
22. Cugnon, J., *Heavy-Ion Collisions*, Bonche, P. *et al.*, Eds., New York: Plenum, 1986, p. 209.
23. Bialas, A. and Peschanski, R., *Nucl. Phys. B*, 1986, vol. 273, p. 703.
24. Ploszajczak, M. and Tucholski, A., *Nucl. Phys. A*, 1991, vol. 523, p. 651.
25. Cugnon, J. and Volant, C., *Z. Phys. A: At. Nucl.*, 1989, vol. 334, p. 435.
26. Cugnon, J., Jasselette, P., and Vandermeulen, J., *Nucl. Phys. A*, 1987, vol. 470, p. 558.
27. Suraud, E., Grégoire, C., and Tamain, B., *Prog. Nucl. Part. Sci.*, 1989, vol. 23, p. 357.
28. Abgrall, P., Haddad, F., De la Mota, V., and Sébille, F., *Phys. Rev. C: Nucl. Phys.*, 1993 (in press).
29. Ngô, C., Abstracts of Papers, *Nuclear Matter and Heavy Ion Collisions*, Soyeur, M. *et al.*, Eds., New York: Plenum, 1989, p. 231.
30. Gross, D.H.E., *Rep. Prog. Phys.*, 1990, vol. 53, p. 605.
31. Cugnon, J., *Nucl. Phys.*, 1989, vol. 8, p. 255.
32. Cugnon, J. (to be published).
33. Hubele, J., Kreutz, P., Adloff, J.C., *et al.*, *Z. Phys. A: At. Nucl.*, 1991, vol. 340, p. 263.
34. Cugnon, J. and L'Hôte, D., *Nucl. Phys. A*, 1986, vol. 452, p. 738.
35. En'yo, H., *Doctorate Dissertation*, Univ. of Tokyo, 1985.
36. Jiang, D.X., Doubre, H., Galin, J., *et al.*, *Nucl. Phys. A*, 1989, vol. 503, p. 560.